

# Repeated Mild Head Injury Leads to Wide-Ranging Deficits in Higher-Order Cognitive Functions Associated with the Prefrontal Cortex

Amber Nolan,<sup>1–3,\*</sup> Edel Hennessy,<sup>1,2,\*</sup> Karen Krukowski,<sup>1,2</sup> Caroline Guglielmetti,<sup>2,4</sup>  
Myriam M. Chaumeil,<sup>2,4</sup> Vikaas S. Sohal,<sup>5</sup> and Susanna Rosi<sup>1,2,6–8</sup>

## Abstract

Traumatic brain injury (TBI) has long been identified as a precipitating risk factor for higher-order cognitive deficits associated with the frontal and prefrontal cortices (PFC). In addition, mild repetitive TBI (rTBI), in particular, is being steadily recognized to increase the risk of neurodegenerative disease. Thus, further understanding of how mild rTBI changes the pathophysiology of the brain to lead to cognitive impairment is warranted. The current models of rTBI lack knowledge regarding chronic higher-order cognitive functions and the underlying neuronal physiology, especially functions involving the PFC. Here, we establish that five repeated mild hits, allowing rotational acceleration of the head, lead to chronic deficits in PFC-dependent functions such as social behavior, spatial working memory, and environmental response with concomitant microgliosis and a small decrease in the adaptation rate of layer V pyramidal neurons in the medial PFC (mPFC). However, structural damage is not seen on *in vivo* T2-weighted magnetic resonance imaging (MRI), and extensive intrinsic excitability changes in layer V pyramidal neurons of the mPFC are not observed. Thus, this rTBI animal model can recapitulate chronic higher-order cognitive impairments without structural damage on MR imaging as observed in humans.

**Keywords:** disinhibition; prefrontal cortex; repetitive mild traumatic brain injury; social memory; working memory

## Introduction

**T**RAUMATIC BRAIN INJURY (TBI) is the leading cause of chronic neurological disability.<sup>1–3</sup> The most common deficits reported even after a mild TBI are in higher-order cognitive functions involving the frontal and prefrontal cortices (PFC).<sup>4–11</sup> Similar behavioral abnormalities, such as increased risk-taking, changes in social behavior, lack of judgment, and mood disorders, are also noted as early symptoms in chronic traumatic encephalopathy (CTE), a neurodegenerative disease associated with repetitive head injury.<sup>12–14</sup> While mild repetitive TBI (rTBI) has been clearly linked with CTE,<sup>15</sup> many other progressive neurodegenerative diseases, including Alzheimer's disease, Parkinson's disease, amyotrophic lateral sclerosis, and multiple sclerosis are additionally associated with TBI.<sup>16–20</sup> Notably, after an initial TBI there is greater vulnerability to subsequent injuries and increased cognitive impairment.<sup>21,22</sup>

For these reasons, investigation of the underlying mechanisms associated with cognitive dysfunction after rTBI is needed. Several models of rTBI have been developed but the chronic cognitive deficits and the underlying neuronal physiology, especially deficits related to PFC function, have not been evaluated. The CHIMERA

(Closed-Head Impact Model of Engineered Rotational Acceleration) model is a newly developed injury device that allows precise control of impact energy, velocity, and direction of injury, while allowing free movement of the head, similar to most types of human TBI.<sup>23,24</sup> With this device, it is possible to deliver multiple, reproducible, mild closed-head injuries.<sup>23,24</sup> Long-lasting hippocampal-dependent learning impairments have been reported up to 6 months after three mild hits<sup>25</sup>; however, the range of chronic maladaptive impairments in higher-order cognitive functions such as those observed in humans after repetitive trauma, as well as the underlying neuronal physiology, are currently unknown.

Using the CHIMERA apparatus, here we investigated PFC-dependent chronic cognitive functions as well as structural T2-weighted MR imaging and the pathophysiology of the PFC after five repetitive mild hits in male mice.

## Methods

### Animal procedures

All animal experiments were conducted in compliance with animal protocols approved by the Institutional Animal Care and

<sup>1</sup>Brain and Spinal Injury Center, <sup>2</sup>Department of Physical Therapy and Rehabilitation Science, <sup>3</sup>Department of Anatomic Pathology, <sup>4</sup>Surbeck Laboratory of Advanced Imaging, Department of Radiology and Biomedical Imaging, <sup>5</sup>Department of Psychiatry, <sup>6</sup>Department of Neurological Surgery, <sup>7</sup>Weill Institute for Neuroscience, <sup>8</sup>Kavli Institute of Fundamental Neuroscience, University of California, San Francisco, San Francisco, California.

\*These two authors contributed equally.

Use Committee at the University of California, San Francisco (UCSF), following National Institutes of Health guidelines for animal care. Because repetitive injury in humans has predominantly been reported in male athletes, particularly in contact sports, and in veterans,<sup>13,26–29</sup> we sought to first specifically evaluate male mice to examine if this model of mild rTBI could recapitulate the higher-order cognitive deficits observed in humans. C57BL/6J male mice were purchased from the Jackson Laboratory at 7 weeks of age. Mice were given one week of acclimation and housed with a reversed 12-h light/12-h dark cycle and provided food and water *ad libitum*. At 8 weeks of age, mice (total  $n=41$ ) were randomly assigned to the rTBI ( $n=19$ ) or sham control group ( $n=22$ ). Animals were anesthetized using isoflurane (2%) in oxygen 1 L/min during the procedure. rTBI animals were subjected to multiple, mild, closed-head injuries using the CHIMERA device as previously reported.<sup>23,24</sup> Briefly, rTBI animals were placed supinely into an angled holding platform without any shaving of the head or incision into the skin so that the head was level with the piston target hole while aligning the eyes, ears, and nose such that the impact was centered on the dorsal convexity of the skull, targeting a 5-mm area surrounding bregma. A nose cone delivering isoflurane was removed just prior to the impact. Impact was initiated using RealTerm software, which was connected to a system including air tank, pressure regulator, digital pressure gauge, two-way solenoid valve, and piston. The impact was administered using an air pressure of 2.95 psi, resulting in an impact energy of 0.5 J from the 5 mm, 50 g piston.<sup>23,24</sup> Animals were moved to an incubator immediately after the impact and monitored until fully recovered. rTBI animals received an injury once per day for 5 days with a 24 h interval in between impacts. Five repeated hits were chosen to specifically focus on the effects of repeated exposure to TBI, as athletes and veterans are exposed to constant and repeated blows, even without experiencing concussive symptoms. Sham mice were exposed to the same isoflurane anesthesia paradigm (~8 min of anesthesia) without sustaining an impact. All animals regained the righting reflex in 5 min or less. Skull fractures, seizures, apnea, or mortality were not observed in any animals, and no animals were excluded from the study due to injury parameters.

Mice underwent behavioral testing between 26 and 35 days post-injury (dpi), elevated plus maze at 26 dpi ( $n=9$ –10/group), social testing on 27–28 dpi ( $n=13$ –16/group), and delayed matching to place (DMP) using a modified Barnes maze at 32–35 dpi ( $n=15$ –18/group). *In vivo* magnetic resonance imaging (MRI) was performed at 40 dpi ( $n=5$ –7/group). These animals were chosen randomly based on MRI scanner availability. In addition, a separate sub-set of animals that did not undergo behavioral testing or *in vivo* imaging ( $n=4$ /group) was used for electrophysiological analysis, with recordings performed at 36–51 dpi. Of note, three separate cohorts of mice were used for testing. The first cohort included 8 sham and 5 rTBI mice and underwent only social and DMP testing. A second cohort included 10 sham and 10 rTBI mice and it was decided to additionally evaluate behavior in the elevated plus maze. A third cohort included 4 sham and 4 rTBI mice and was used only for electrophysiology.

### Behavioral assays

For all behavioral assays the experimenters were blinded to the treatment. Beginning one week prior to behavioral analysis, animals were handled for habituation to experimenters and room settings. Behavior testing was performed during the animals' wake cycle. All behaviors were recorded using an overhead camera connected to a video tracking and analysis system (Ethovision XT 12.0, Noldus Information Technology). When tracking was not optimal, videos were manually scored by an investigator blinded to the treatment.

**Elevated plus maze (EMP).** At 26 dpi, animals were tested for their response to environmental stimuli using an elevated plus-

shaped maze ( $n=9$ –10/group) raised 40 cm above the floor in a room with bright lighting, as previously described.<sup>30–32</sup> The surface of the maze consisted of two closed arms opposite each other (30.5 cm in length) enclosed in black plastic. The other two perpendicular arms were open (35 cm in length) with white lights illuminating the open arms. Mice were placed in the center (4.5 cm square) of the maze and allowed to explore for 5 min while their location and activity were recorded. The maze was cleaned with 70% ethanol between animals. The time in the open (which included time both in the open arms and center, which is uncovered) as well as the total distance traveled for each animal were recorded and scored using a video tracking and analysis setup (Ethovision XT 8.5, Noldus Information Technology). One sham animal fell off the maze during testing and was excluded from analysis.

**Sociability and social memory.** At 27–28 dpi, sociability and social memory were assessed using a three-chamber social approach task in a dark room under red lighting as previously described ( $n=13$ –16/group).<sup>32,33</sup> Animals were placed individually into the center of the three chambers and their behavior was recorded during three consecutive phases: habituation, sociability, and social memory. In the habituation phase, the test animal was allowed to explore all three chambers for 10 min. In the sociability phase, the mouse was returned to the center chamber while the experimenter placed a novel (non-aggressive, sex- and aged-matched) mouse in a wire cage on one side. On the opposite side, an empty wire cage was present (schematic in Fig. 2A). The test animal was allowed to explore for 10 min. In the social memory phase, the test animal was once again returned to the center chamber. In the previously empty wire cage, a novel (non-aggressive, sex- and aged-matched) mouse was placed, while the now familiar mouse was left in the opposite wire cage (schematic in Fig. 2D). The test subject was then given 5 min to explore. All of the apparatus was thoroughly cleaned using 70% ethanol between each animal. Animals were excluded from analysis if they failed to explore (less than 5 sec of interaction) either the novel mouse or the empty cage/familiar mouse. Animals that failed to explore during the sociability phase were also excluded from the social memory phase.

**Delayed matching to place (DMP).** Spatial working memory was evaluated at 32–35 dpi using a modified Barnes maze (pictured in Fig. 3A) in a room with bright lighting, as previously described ( $n=15$ –18/group).<sup>34</sup> The maze consisted of a round table 112 cm in diameter with 40 escape holes arranged in three concentric rings consisting of 8, 16, and 16 holes at 20, 35, and 50 cm from the center of the maze, respectively. An escape tunnel was connected to one of the outer holes. Two visual cues were placed around the room such that they were visible to animals on the table. Bright overhead lighting and a loud tone (2 KHz, 85 db) were used as aversive stimuli to motivate animals to locate the escape tunnel. The assay was performed for 4 days (32–35 dpi). The escape tunnel location was moved each day and animals ran four trials per day.

During each trial, animals were placed onto the center of the table covered by a dark box to prevent exposure to the room. The start of the trial was initiated when the box was removed and the tone started playing. The trial ended when the animal reached the escape tunnel or a maximum trial time of 90 sec was reached. Upon entry into the tunnel, the tone was stopped. Animals that failed to find the escape tunnel were guided there. Animals remained in the escape tunnel for 10 sec before being returned to their home cage. The maze and escape tunnel were cleaned with ethanol between each trial. No animals were excluded from this analysis.

### *In vivo* magnetic resonance imaging acquisitions

MRI was performed on a 14.1 Tesla vertical MR system (Agilent Technologies, Palo Alto, CA) equipped with 100 G/cm gradients and a 1 H volume coil (internal diameter  $\varnothing I=40$  mm). At 40 dpi, mice ( $n=5$ –7/group) were anesthetized using isoflurane (2% in O<sub>2</sub>)

and then placed in a cylindrical holder with a tooth bar, allowing for reproducible positioning of the mouse head. Throughout all acquisitions, respiration rate and body temperature were continuously monitored. High-resolution axial T<sub>2</sub>-weighted fast spin echo images of the entire brain were acquired using the following parameters: Echo time (TE)/repetition time (TR) = 11.6/2006 msec, echo train = 8, slice thickness = 0.5 mm, slice number = 20, number of averages = 2, matrix = 256 × 256, field of view (FOV) = 30 × 30 mm<sup>2</sup>, scanning time = 2 min, 12 sec.

### Magnetic resonance image analysis

For anatomical and structural analyses, regions of interest including the corpus callosum, cortex, hippocampus, ventricles, and total brain were manually delineated utilizing AMIRA<sup>®</sup> software (Mercury Computer Systems, San Diego) as depicted in Supplementary Figures 1 and 2 (see online supplementary material at <http://www.liebertpub.com>). For each region of interest, volume and regional average of T<sub>2</sub>-weighted MR signals, normalized to the average signal from the cerebral spinal fluid of the lateral and third ventricles (nT<sub>2w</sub>), were computed.

### Electrophysiology

Coronal brain slices (250 μm) including the medial PFC (mPFC) were prepared from both sham and rTBI mice, 36–51 dpi (*n* = 4/group). Mice were anesthetized with Euthosal<sup>®</sup> (0.1 mL/25 g), and transcardially perfused with an ice-cold sucrose cutting solution containing (in mM): 210 sucrose, 1.25 NaH<sub>2</sub>PO<sub>4</sub>, 25 NaHCO<sub>3</sub>, 2.5 KCl, 0.5 CaCl<sub>2</sub>, 7 MgCl<sub>2</sub>, 7 dextrose, 1.3 ascorbic acid, 3 sodium pyruvate (bubbled with 95% O<sub>2</sub>–5% CO<sub>2</sub>, pH ~7.4). Mice were then decapitated and the brain was isolated in the same sucrose solution, and cut on a slicing vibratome. Slices were incubated in a holding solution (composed of [in mM] 125 NaCl, 2.5 KCl, 1.25 NaH<sub>2</sub>PO<sub>4</sub>, 25 NaHCO<sub>3</sub>, 2 CaCl<sub>2</sub>, 2 MgCl<sub>2</sub>, 10 dextrose, 1.3 ascorbic acid, 3 sodium pyruvate, bubbled with 95% O<sub>2</sub>–5% CO<sub>2</sub>, pH ~7.4) at 36°C for 30 min and then at room temperature for at least 30 min until recording.

Whole cell current-clamp recordings were obtained from these slices in a submersion chamber with a heated (32–34°C) artificial cerebrospinal fluid (aCSF) containing (in mM): 125 NaCl, 3 KCl, 1.25 NaH<sub>2</sub>PO<sub>4</sub>, 25 NaHCO<sub>3</sub>, 2 CaCl<sub>2</sub>, 1 MgCl<sub>2</sub>, 10 dextrose (bubbled with 95% O<sub>2</sub>–5% CO<sub>2</sub>, pH ~7.4). Patch pipettes (3–6 MΩ) were manufactured from filamented borosilicate glass capillaries and filled with an intracellular solution containing (in mM): 135 KGlucuronate, 5 KCl, 10 HEPES, 4 NaCl, 4 MgATP, 0.3 Na<sub>3</sub>GTP, 7 2K-phosphocreatine, and 0.5–1% biocytin or neurobiotin. Layer V pyramidal neurons in the mPFC were identified using infrared microscopy with a 40x water-immersion objective (Olympus, Burlingame, CA). Recordings were made using a Multiclamp 700B (Molecular Devices, Sunnyvale, CA) amplifier, which was connected to the computer with a Digidata 1320 ADC, and recorded at a sampling rate of 10–20 kHz with pClamp<sup>™</sup> software (Axon Instruments, Sunnyvale, CA). We did not correct for the junction potential, but access resistance and pipette capacitance were appropriately compensated before each recording. Only neurons with an access resistance <20 MΩ and a resting membrane potential below –55 mV were included.

The membrane and spiking characteristics were assessed by injection of a series of hyperpolarizing and depolarizing current steps with a duration of 250 msec from –250 pA to 700 nA (in increments of 50 pA). The resting membrane potential was the measured voltage of the cell 5 min after obtaining whole cell configuration without current injection. A holding current was then applied to maintain the neuron at –70 mV before/after current injections. The input resistance was determined from the steady-state voltage reached during the –50 pA current injection. The membrane time

constant was the time required to reach 63% of the maximum change in voltage for the –50 pA current injection. The degree of I<sub>H</sub> current was assessed by measuring two parameters: 1) the voltage sag, defined as the change in voltage between the maximum hyperpolarization and the steady state potential for the –200 pA current injection; and 2) the rebound after depolarization (ADP), defined as the change in voltage between the maximum depolarization and the steady-state potential achieved immediately after ending the –200 pA current injection. The sum of these two variables is an overall indicator of the amount of I<sub>H</sub> current.<sup>35</sup> Action potential parameters were measured from the current injection that was 100 pA above the first current injection that elicited spiking, or if this injection had fewer than 3 action potentials, the first current injection with >3 action potentials. Action potential times were detected by recording the time at which the positive slope of the membrane potential crossed 0 mV. From the action potential times, the instantaneous frequency for each action potential was determined (1/inter spike interval). Action potential rate as a function of current injection was examined by plotting the first instantaneous action potential frequency versus current injection amplitude. The F/I slope was then determined from the best linear fit of the positive values of this plot. The action potential amplitude was calculated by measuring the voltage difference between the peak voltage of the action potential and the subsequent minimum voltage prior to the next action potential. The half width of the action potential was determined as the average duration of the action potentials at half the amplitude. The frequency adaptation of each cell was the ratio of the first over the last instantaneous firing frequency. Action potential threshold was defined as the voltage at the maximum second derivative of V ( $d^2V/dt$ ) in the phase-space representation of the action potential.<sup>36</sup>

### Immunohistochemistry

Brain slices obtained from electrophysiological recordings were drop-fixed in 4% paraformaldehyde in a phosphate-buffered solution (4–48 h), then rinsed with phosphate-buffered saline (PBS) with sodium azide (0.1 M PBS + 0.05% NaN<sub>3</sub>) and stored at 4°C for 0–5 days until processing. Sections were then washed in PBS (3 × 10 min), incubated in a blocking solution (10% donkey serum diluted in 0.5% Triton X-100 in 0.1M PBS) for 1 h, and then incubated with primary antibody, IBA-1 (1:500, Wako 019-19741) with 0.25% Triton X-100, and 5% donkey serum in 0.1 M PBS, at room temperature overnight, along with a streptavidin-conjugated Alexafluor 555 (1:500, ThermoFisher Scientific, S32355). The following day, sections were then rinsed with PBS (3 × 10 min) and incubated in secondary antibody (1:500, Alexa 488 donkey anti-rabbit, Invitrogen, A21206) at room temperature overnight. Finally, sections were rinsed and mounted in an aqueous medium. Images were obtained using a Zeiss Imager Z1 Apotome microscope controlled by ZEN software (Zeiss 2012). For each mouse, three sections of mPFC (from bregma 1.42–1.98 mm) were imaged with a 20x objective, centered over layer V and including multiple layers of cortex (~ layers II–VI), obtaining a Z-stack of 10 μm with a 0.5-μm slice interval. Image stacks were viewed and Z-projected using ImageJ (National Institutes of Health, Bethesda, MD) or LSM Viewer (Zeiss). IBA-1-positive cells were manually counted for each image and divided by the total surface area of the flattened image to obtain the number of cells/mm<sup>2</sup>.

### Statistical analysis

All data were analyzed with GraphPad Prism 7 statistical software. It is well established that violations in normality have little effect on Type I error rates,<sup>37</sup> therefore we have used a very restricted definition for defining data as non-parametric: using both D'Agostino-Pearson omnibus and Shapiro-Wilk tests, the data distribution had to exhibit an alpha <0.01 for both tests to be considered outside of the normal distribution. Differences in

variance between groups were determined using an F test. Statistical significance between groups for most variables was determined using a two-tailed *t* test. If there was a significant difference in variance between groups, Welch's correction was added to the two-tailed *t* test. If data were outside of the normal distribution as indicated above, a nonparametric Mann-Whitney U test was used. The DMP maze and the firing response to increasing current injections were analyzed as a repeated measures two-way analysis of variance (ANOVA) with a Bonferroni post hoc examination. Outliers were determined using the extreme Studentized deviate (ESD) method and were excluded from analysis. *P* values <0.05 were considered significant.

## Results

### Repetitive mild traumatic brain injury and risk-taking phenotype

To examine if mice exposed to rTBI responded to environmental stimuli differently, we evaluated risk-taking phenotype using the elevated plus maze, in which mice freely explore either two closed, dark arms or two open, illuminated arms. Mice that received rTBI spent a significantly longer time in the open compared with the sham animals, 26 dpi ( $F_{(9,8)}=2.91$ ,  $p<0.05$ ;  $h^2=0.27$ ; two-tailed *t* test; Fig. 1A). This phenotype suggests behavioral disinhibition or an increased risk-taking phenotype. Notably, these effects were not explained by differences in activity levels, as both groups traveled a similar distance in the maze ( $F_{(9,8)}=2.82$ ,  $p=0.14$ ;  $h^2=0.07$ ; two-tailed *t* test; Fig. 1B).

### Repetitive mild traumatic brain injury and social behaviors

Using the three-chamber social task, we next investigated the effect of rTBI on social function at 27–28 dpi.<sup>32,33</sup> In this task, sociability is measured by an animal's preference for social interaction over an empty cage, calculated by the preference ratio (time with the mouse/time with the empty cage). No differences in sociability ( $F_{(15,12)}=1.06$ ,  $p=0.15$ ;  $h^2=0.08$ ; two-tailed *t* test; Fig. 2B) or total interaction time with the mouse or empty cage were measured between the sham and rTBI animals ( $F_{(15,12)}=1.06$ ,  $p=0.38$ ;  $h^2=0.03$ ; two-tailed *t* test; Fig. 2C). Next, we tested social memory, which is the ability for the animal to distinguish a novel mouse from a previously exposed animal calculated by the preference ratio (time with novel mouse/time with familiar mouse). Animals that received five repetitive mild injuries had significantly less interaction with the novel animal in comparison with the sham group ( $F_{(15,11)}=1.34$ ,

$p<0.05$ ;  $h^2=0.16$ ; two-tailed *t* test; Fig. 2D). This significant reduction in the novel/familiar preference ratio is indicative of impairment in social memory. Overall, mice were still able to recognize the novel mouse compared with the familiar mouse, with a novel/familiar mouse ratio significantly greater than 1 ( $2.307 \pm 0.4383$  preference ratio in rTBI; one-sample  $t_{(11)}=2.98$ ,  $p<0.05$ ; one-sample *t* test). Total interaction time with the novel and familiar mouse ( $F_{(11,15)}=1.32$ ,  $p=0.1371$ ;  $h^2=0.08$ ; two-tailed *t* test; Fig. 2E) was not significantly different between groups, suggesting that social impairments were not due to decreased interest in the task.

### Spatial working memory after repetitive mild traumatic brain injury

Lastly, we evaluated spatial working memory and learning after rTBI with the delayed matching to place (DMP) dry maze test at 32–35 dpi.<sup>34</sup> Using visual cues, animals learn to locate an escape tunnel attached to one of 40 holes in a circular table to evade loud noise in a brightly lit room. Importantly, the escape location is changed every day, forcing the animal to relearn the location of the tunnel, thus providing an assessment of spatial working memory. To quantify performance, Ethovision tracking software measures the “escape latency,” which is the time taken for the mouse to enter the escape tunnel after being placed in the maze. By the end of day 3, sham animals learned to locate the escape tunnel faster than rTBI animals. ( $F_{(1,31)}=12.83$ ,  $p<0.01$ ;  $h^2=0.05$  for treatment effect.  $F_{(15,465)}=14.55$ ,  $p<0.001$ ;  $h^2=0.24$  for trial effect.  $F_{(15,465)}=1.95$ ,  $p<0.05$ ;  $h^2=0.03$  for treatment x trial interaction, repeated measures 2-way ANOVA. After correcting for multiple comparisons, trials 2, 3, and 4 on day 3 [ $p<0.05$ ] and trial 3 on day 4 [ $p<0.001$ ] show significant elevated escape latency in rTBI mice compared with sham mice; Bonferroni post hoc test; Fig. 3B.) Additionally, sham animals exhibited spatial learning (defined by a significant reduction in escape latency between trial 1 and trial 4 using a Bonferroni post hoc test with repeated measure two-way ANOVA testing) by day 2 ( $p<0.001$ ), which continued through day 4 (day 3  $p<0.001$ ; day 4  $p<0.0001$ ), whereas rTBI animals only demonstrated learning on day 4 ( $p<0.01$ ). The elevated escape latency compared with sham mice and lack of learning until day 4 observed in rTBI mice compared with day 2 in sham mice is indicative of impaired spatial working memory. Averages of the four trials per day also revealed significant differences between the sham and rTBI mice on days 3 and 4 of testing. ( $F_{(1,31)}=16.84$ ,  $p<0.001$ ;  $h^2=0.12$  for treatment effect.  $F_{(3,93)}=20.71$ ,  $p<0.0001$ ;  $h^2=0.24$  for day effect.  $F_{(3,93)}=2.01$ ,  $p<0.05$ ;  $h^2=0.03$  for treatment x day interaction,

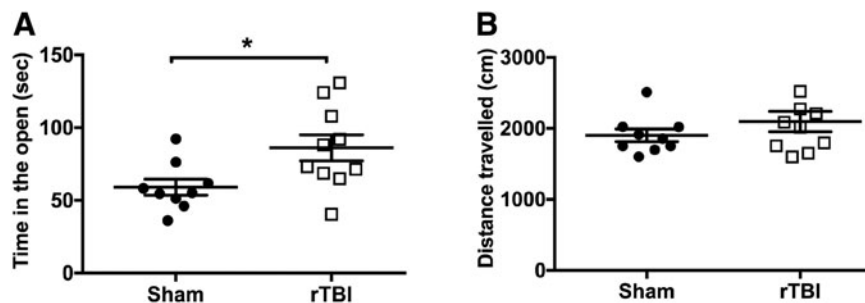


**FIG. 1.** rTBI causes behavioral disinhibition in the elevated plus maze, 26 dpi. (A) Time spent in the open areas of the maze is increased in rTBI compared with sham mice. Data are mean  $\pm$  SEM ( $F_{(9,8)}=2.91$ ,  $*p<0.05$ ;  $h^2=0.27$ ; two-tailed *t* test). (B) The distance traveled during the elevated plus maze task is similar between groups. Data are mean  $\pm$  SEM ( $F_{(9,8)}=2.82$ ,  $p=0.14$ ;  $h^2=0.07$ ; two-tailed *t* test). ( $n=9$ –10/group.) rTBI, repetitive traumatic brain injury; SEM, standard error of the mean.

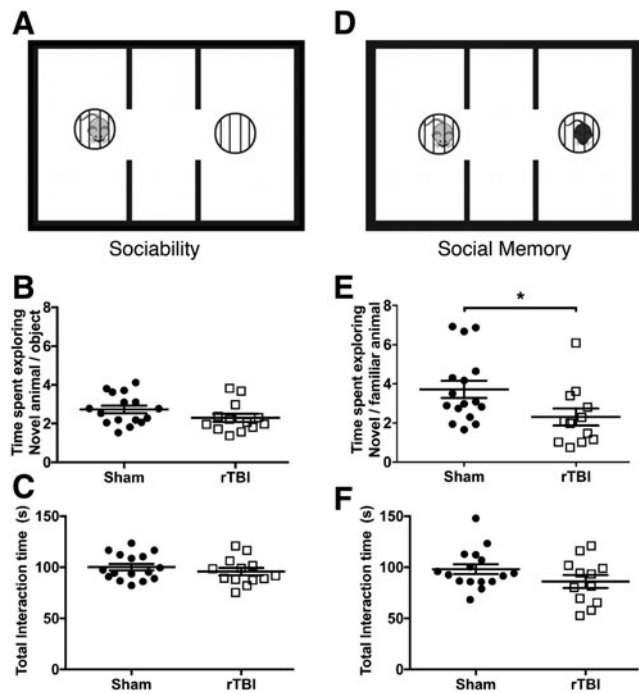


**FIG. 2.** rTBI effects social functions, 27–28 dpi. (A) Schematic of the three-chamber sociability task. Mice were exposed to a novel mouse (left chamber, light gray) and a novel object: empty cage (right chamber). (B) Proportion of time spent exploring the novel mouse over the novel object is comparable in both rTBI and sham mice. Data are mean  $\pm$  SEM ( $F_{(15,12)}=1.06$ ,  $p=0.15$ ;  $h^2=0.08$ ; two-tailed  $t$  test). (C) Total interaction time with either the novel object or mouse is similar between groups. Data are mean  $\pm$  SEM ( $F_{(15,12)}=1.06$ ,  $p=0.38$ ;  $h^2=0.03$ ; two-tailed  $t$  test). (D) Schematic of the three-chamber social memory task. Mice were exposed to the same (now familiar) mouse from the sociability phase (left chamber, light gray) and a new novel mouse (right chamber, black). (E) Proportion of time spent exploring the novel mouse over the familiar mouse is decreased in rTBI mice compared with sham mice. Data are mean  $\pm$  SEM ( $F_{(15,11)}=1.34$ ,  $*p<0.05$ ;  $h^2=0.16$ ; two-tailed  $t$  test). (F) Total interaction time with either the novel or familiar mouse is similar between groups. Data are mean  $\pm$  SEM ( $F_{(11,15)}=1.32$ ,  $p=0.1371$ ;  $h^2=0.08$ ; two-tailed  $t$  test). ( $n=13$ – $16$ /group.) rTBI, repetitive traumatic brain injury; SEM, standard error of the mean.

repeated measures two-way ANOVA; day 3/34 dpi  $p<0.001$  and day 4/35 dpi  $p<0.01$ ; Bonferroni post hoc test; Fig. 3C,D.)

#### MRI and repetitive mild traumatic brain injury

Despite the wide-ranging deficits in behavior, *in vivo*  $T_2$ -weighted MRI analysis did not find changes in the anatomical volumes or the  $nT_2w$  signal throughout the cortex, hippocampus, or white matter structures (results detailed in Supplementary Figs. 1 and 2; see online supplementary material at <http://www.liebertpub.com>). Notably, these findings are congruent with human data, where disabling cognitive deficits after repetitive injury are not associated with MRI findings.<sup>38,39</sup>

#### Intrinsic excitability of mPFC layer V pyramidal neurons after repetitive mild traumatic brain injury

Given that the mPFC is a brain region important in integration of complex behavior and required for proper working memory,<sup>40</sup> social

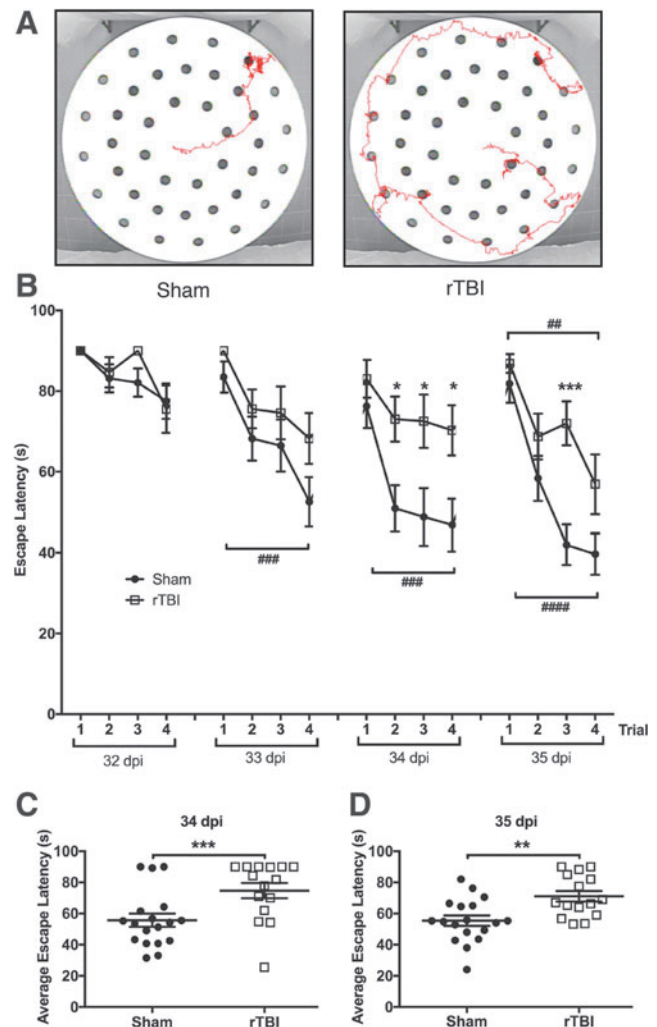


**FIG. 3.** rTBI impairs spatial learning and working memory, 32–35 dpi. (A) Representative activity tracks for the last trial of a sham animal (left panel) and rTBI animal (right panel). (B) rTBI mice exhibit an altered escape latency compared with sham mice, most prominently on days 3 and 4 of testing. In addition, sham mice appear to learn by day 2 with a significant difference between trial 1 and 4, whereas rTBI mice do not demonstrate learning until day 4. Data are mean  $\pm$  SEM ( $F_{(1,31)}=12.83$ ,  $p<0.01$ ;  $h^2=0.05$  for treatment effect,  $F_{(15,465)}=14.55$ ,  $p<0.001$ ;  $h^2=0.24$  for trial effect,  $F_{(15,465)}=1.95$ ,  $p<0.05$ ;  $h^2=0.03$  for treatment  $\times$  trial interaction, repeated measures two-way ANOVA); trials 2, 3, and 4 on day 3 ( $*p<0.05$ ) and trial 3 on day 4 ( $***p<0.001$ ) show significant elevated escape latency in rTBI mice compared with sham mice; a significant reduction in escape latency between trial 1 and trial 4 is identified in sham mice on day 2 ( $####p<0.001$ ), which continued through day 4 (day 3  $####p<0.001$ ; day 4  $####p<0.0001$ ), whereas rTBI animals only demonstrated a significant reduction in escape latency between trial 1 and trial 4 on day 4 ( $##p<0.01$ ; Bonferroni post hoc test). Individual animal performances averaged across trials 1–4 on days 3 (C) and 4 (D) of the DMP (34 and 35 dpi). rTBI animals were significantly slower at locating the escape location compared with sham animals. Data are means  $\pm$  SEM ( $F_{(1,31)}=16.84$ ,  $p<0.001$ ;  $h^2=0.12$  for treatment effect,  $F_{(3,93)}=20.71$ ,  $p<0.0001$ ;  $h^2=0.24$  for day effect,  $F_{(3,93)}=2.01$ ,  $p<0.05$ ;  $h^2=0.03$  for treatment  $\times$  day interaction, repeated measures two-way ANOVA; day 3/34 dpi  $***p<0.001$  and day 4/35 dpi  $**p<0.01$ ; Bonferroni post hoc  $t$  test). ( $n=15$ – $18$ /group.) ANOVA, analysis of variance; rTBI, repetitive traumatic brain injury; SEM, standard error of the mean. Color image is available online at [www.liebertpub.com/neu](http://www.liebertpub.com/neu)

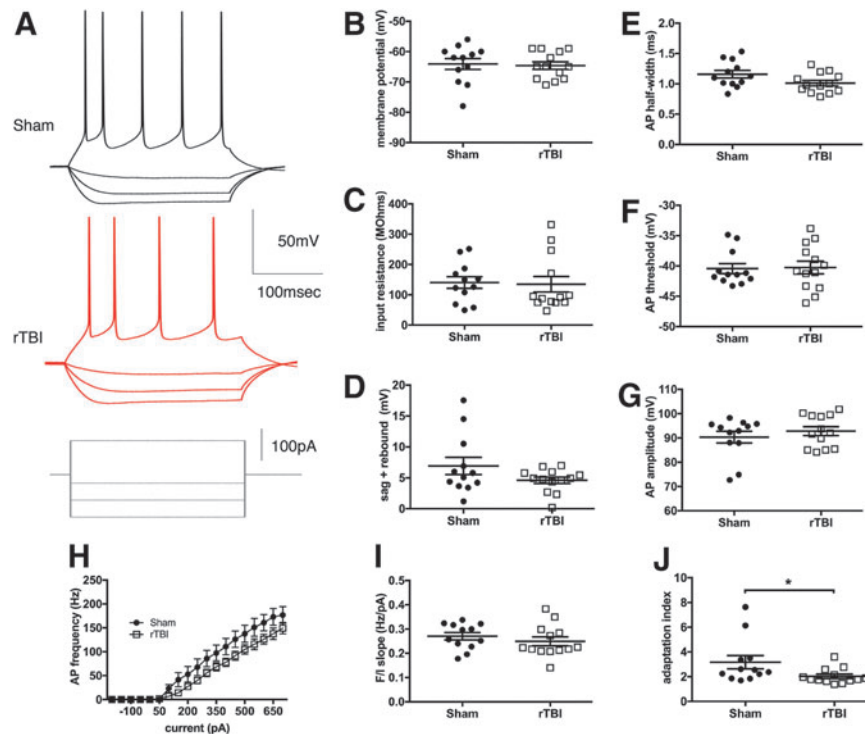


**FIG. 4.** Intrinsic excitability of layer V pyramidal neurons in the mPFC is minimally altered after rTBI. (A) Representative traces from layer V pyramidal neurons showing the membrane potential response to current injection ( $-250$ ,  $-150$ ,  $-50$ ,  $200$  pA). Analysis of the passive membrane properties showed no significant difference between sham and rTBI groups for the resting membrane potential (B,  $F_{(11,12)}=2.00$ ,  $p=0.81$ ;  $h^2=0.003$ ; two-tailed  $t$  test) or input resistance (C,  $F_{(12,11)}=1.96$ ,  $p=0.87$ ;  $h^2=0.001$ ; two-tailed  $t$  test). The sum of the sag, and rebound response, indicative of the amount of  $I_H$  current, was not altered (D,  $F_{(11,12)}=6.57$ ,  $p=0.14$ ;  $h^2=0.15$ ; two-tailed  $t$  test with Welch's correction). A non-significant trend for a reduction in action potential (AP) half width was noted in the rTBI group (E,  $F_{(11,12)}=1.74$ ,  $p=0.07$ ;  $h^2=0.14$ ; two-tailed  $t$  test); however, the AP threshold (F,  $F_{(12,11)}=1.75$ ,  $p=0.89$ ;  $h^2=0.001$ ; two-tailed  $t$  test) and AP amplitude (G,  $F_{(11,12)}=1.60$ ,  $p=0.42$ ;  $h^2=0.03$ ; two-tailed  $t$  test) were similar between groups. There was a trend for a decreased initial instantaneous frequency of firing with rTBI, which was not significant with repeated measures two-way ANOVA testing (H,  $F_{(1,23)}=2.86$ ,  $p=0.10$ ;  $h^2=0.02$  for rTBI treatment effect, repeated measures two-way ANOVA). The slope of the relationship between current injection and AP frequency response (I,  $F_{(12,11)}=1.53$ ,  $p=0.39$ ;  $h^2=0.03$ ; two-tailed  $t$  test) was not different. However, a reduction in the adaptation of the AP interval over time was identified in the rTBI group compared with the sham group (J, Mann-Whitney  $U=37$ ,  $*p<0.05$  two-tailed). All data are mean  $\pm$  SEM. ( $n=4$  animals/group with 3–4 cells per animal). ANOVA, analysis of variance; mPFC, medial prefrontal cortex; rTBI, repetitive traumatic brain injury; SEM, standard error of the mean. Color image is available online at [www.liebertpub.com/neu](http://www.liebertpub.com/neu)

function,<sup>41</sup> and contextual or environmental response,<sup>42</sup> we sought to evaluate for possible changes in intrinsic excitability of layer V pyramidal neurons in this region after rTBI. Layer V was specifically chosen for evaluation as it is the primary output layer of the cortical microcircuit. We closely examined the neuronal response to a series of hyperpolarizing and depolarizing current steps (20 steps from  $-250$  to  $700$  pA,  $250$  msec duration). There were no significant differences in the majority of passive and active properties of the neuron (Fig. 4) between sham and rTBI groups; however, a small difference was identified in the adaptation index as discussed below. Resting membrane potential ( $F_{(11,12)}=2.00$ ,  $p=0.81$ ;  $h^2=0.003$ ; two-tailed  $t$  test), input resistance ( $F_{(12,11)}=1.96$ ,  $p=0.87$ ;  $h^2=0.001$ ; two-tailed  $t$  test), and the  $I_H$  current effect (measured as the sum of the sag and rebound;  $F_{(11,12)}=6.57$ ,  $p=0.14$ ;  $h^2=0.15$ ; two-tailed  $t$  test with Welch's correction) were equivalent in both groups (Fig. 4B–D). Action potential indices were not significantly altered, including the amplitude ( $F_{(11,12)}=1.60$ ,  $p=0.42$ ;  $h^2=0.03$ ; two-tailed  $t$  test) and the threshold ( $F_{(12,11)}=1.75$ ,  $p=0.89$ ;  $h^2=0.001$ ; two-tailed  $t$  test; Fig. 4F–G), although there was a small non-significant trend for a shorter action potential duration as measured by the half-width for the rTBI group ( $F_{(11,12)}=1.74$ ,  $p=0.07$ ;  $h^2=0.14$ ; two-tailed  $t$  test; Fig. 4E). There was also a trend for a lower initial action potential

frequency response to current injection in the rTBI group compared with sham animals ( $F_{(1,23)}=2.86$ ,  $p=0.10$ ;  $h^2=0.02$  for rTBI treatment effect, repeated measures two-way ANOVA; Fig. 4H), but no differences were noted in the slope of the relationship between the first instantaneous frequency response and current injection amplitude ( $F_{(12,11)}=1.53$ ,  $p=0.39$ ;  $h^2=0.03$ ; two-tailed  $t$  test; Fig. 4I). The only active property with a significant difference between groups was the finding of a lower adaptation rate in the rTBI group, corresponding to the rTBI layer V pyramidal neurons appearing less likely to respond with an initial doublet of spikes as seen in the sham neurons (Mann-Whitney  $U=37$ ,  $p<0.05$  two-tailed; Fig. 4A,J).

Our findings suggest that intrinsic excitability in layer V pyramidal neurons of the mPFC as a whole is not significantly altered 4–6 weeks after rTBI; however, a modest decrease in the adaptation index is noted after rTBI.

#### Microgliosis after repetitive mild traumatic brain injury

To evaluate for chronic microgliosis in the mPFC, we quantified the density of IBA-1-positive cells over layers II through VI of the cortex. The density of IBA-1-positive cells was significantly increased in rTBI mice compared with sham ( $F_{(11,11)}=2.06$ ,

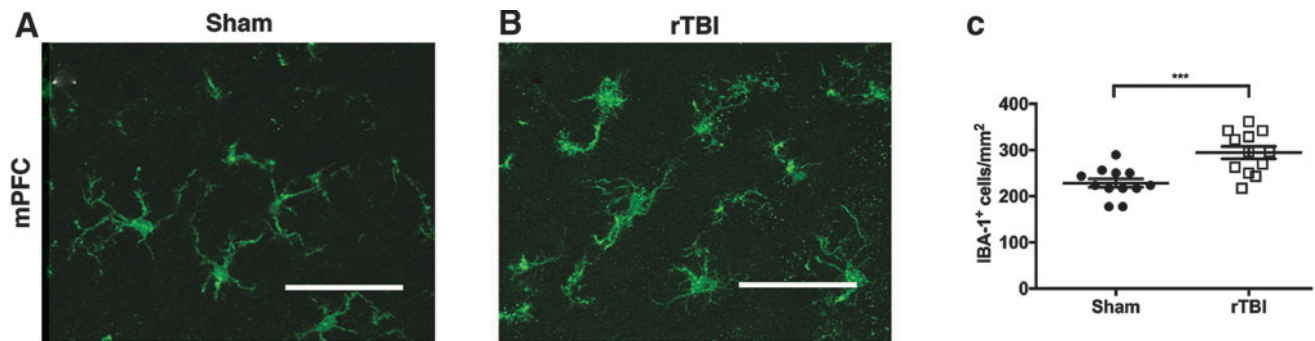


**FIG. 5.** Microgliosis in the mPFC 40 dpi after rTBI. (A) Representative IBA-1 immunostaining in the mPFC of a sham mouse. (B) Representative IBA-1 immunostaining in the mPFC of a rTBI mouse. (C) The density of IBA-1-positive cells/mm<sup>2</sup> is significantly increased in rTBI compared with sham mice. Data are mean  $\pm$  SEM ( $F_{(11,11)} = 2.06$ ,  $***p < 0.001$ ;  $h^2 = 0.43$ ; two-tailed  $t$  test;  $n = 4$  mice [and three sections per mouse]/group). Scale bar = 50  $\mu$ m. mPFC, medial prefrontal cortex; rTBI, repetitive traumatic brain injury; SEM, standard error of the mean. Color image is available online at [www.liebertpub.com/neu](http://www.liebertpub.com/neu)

$p < 0.001$ ;  $h^2 = 0.43$ ; two-tailed  $t$  test; Fig. 5A–C). Similar findings were identified in CA1 of the hippocampus, with an increase in IBA-1 staining in rTBI compared with sham tissue (results detailed in Supplementary Fig. 3; see online supplementary material at <http://www.liebertpub.com>).

## Discussion

In this study, we demonstrated that five consecutive mild head injuries, spaced 24 h apart, lead to chronic higher-order cognitive dysfunction involving multiple modalities that require PFC function in male mice. Specifically, several weeks after rTBI, mice exhibited increased time in the open arms in the elevated plus maze suggestive of behavioral disinhibition or increased risk taking, deficits in social memory, and impaired spatial working memory. These chronic cognitive deficits were associated with microgliosis and a small decrease in the adaptation rate of layer V pyramidal neurons in the mPFC, but no significant changes were measured on T<sub>2</sub>-weighted MRI.

Notably, this model of rTBI may deliver repeated sub-concussive blows. Although we did not specifically test for differences in the acute neurobehavioral response right after impact, prior studies of CHIMERA-induced injury using these same parameters have established that the kinetics these mice experience may be less than the average impact energy experience by NFL players during a concussive blow.<sup>23,24</sup> Further, structural damage is not identified on *in vivo* MRI, similar to human studies of rTBI.<sup>38,39</sup> Given the increasing evidence that repetitive mild hits without associated concussive symptoms can still mediate chronic brain damage and cognitive deficits,<sup>43</sup> the current data suggest that this may represent a valuable and highly needed pre-clinical animal model of repetitive sub-concussive injury.

Social deficits are often studied as a component of psychiatric diseases such as autism and schizophrenia. However, numerous reports show that TBI in humans can lead to many psychiatric symptoms, including a prominent decrease in social function, ability to recognize emotion, and difficulty with family interaction.<sup>44,45</sup> The degree of deficits in social function may even be a predictor of overall functional outcome in these patients.<sup>46</sup> Despite this prominence, only two studies have evaluated social behavior after rTBI. Klemenhagen and colleagues found a decreased response to social novelty 1.5 weeks after two concussive closed-head injuries,<sup>47</sup> whereas Yu and associates identified decreased

social interaction time 3 weeks after five repeated closed-head injuries.<sup>48</sup> However, we are the first to report that deficits in social memory specifically can persist at a chronic time-point ( $\sim 1$  month after injury) after five repeated mild injuries that allow head movement. It is noteworthy that injured mice still recognize the novel mouse (with a ratio of time spent with novel/familiar mouse significantly  $>1$ ) suggesting that a degree of social memory formation may be intact. The lack of anxiety-like behavior in the elevated plus maze task as well as the similar levels of sociability in sham and rTBI groups suggest that the deficits in social memory are not related to social anxiety. Further investigation is required to understand if these social deficits may be secondary to a diminished response to social novelty.

Patients who experience moderate to severe TBI develop disinhibited behaviors such as impulsivity and poor cognitive control lasting  $>6$ –12 months after injury<sup>49</sup>; in addition, disinhibited symptoms are some of the first symptoms noted in athletes with a history of mild rTBI who go on to develop CTE.<sup>12–14</sup> Using the elevated plus maze here we report that mice exposed to repetitive injury spent more time in the open or “aversive” arms compared with sham mice, suggesting increased levels of behavioral disinhibition. These findings are in line with previous animal studies of repetitive head injury that also did not use a stereotactic frame to fix the mouse head.<sup>50–53</sup> However, not all models of repetitive injury exhibited such disinhibition. Yang and co-workers found the opposite relationship with more time in the closed rather than open arms at 30 and 60 days after four repetitive injuries with a fixed head position given  $>3$  days apart.<sup>54</sup> Others have found no difference in response to environmental stimuli after two angular frontal impacts in a diffuse injury model given 48 h apart.<sup>55</sup> These discrepancies might be due to different factors such as the severity of the injury, the total number of injuries, or the exact timing between hits, which are all likely to change the relative degree of neuronal damage in the brain and might correlate to whether mice show more disinhibition or more anxiety. Furthermore, an increased degree of rotational free movement of the head during injury could change the pattern of injury and perhaps lead to increased white matter damage and different behavioral phenotypes that might better mimic the findings that occur during human TBI.

Chronic dysfunction in spatial reference memory is commonly reported in different models of rTBI as measured by the Morris water maze<sup>25,51,54,56,57</sup> and Barnes maze.<sup>50,53,55</sup> Here we used a dry version of a delayed matching to place test by modifying the

Barnes maze task, which requires the animals to relearn a new escape location every day. This additional component assesses working memory,<sup>58</sup> requiring not only the hippocampus, but also prefrontal cortical function.<sup>34</sup> We established that mice specifically exhibit chronic deficits in spatial working memory, not just spatial reference memory. This finding recapitulates the chronic deficits observed in human TBI after a range of mild to severe injury<sup>59–61</sup> and in athletes with CTE,<sup>12–14</sup> and further supports the relevance of this repetitive injury model for studying human disease.

The mPFC is critically involved in many complex neurological and psychiatric behaviors<sup>62</sup> including the behaviors tested here: working memory,<sup>40</sup> social memory,<sup>41</sup> and environmental or contextual response.<sup>42</sup> The mPFC is thought to be a central circuit integrating numerous sensory modalities. Its dense interconnectivity with the hippocampus, striatum, thalamus, and other cortical areas may make this region more vulnerable to the diffuse axonal injury that often accompanies TBI. Indeed, human studies have identified decreased activity on functional MRI (fMRI) in the PFC,<sup>63</sup> loss of connectivity between the hippocampus and mPFC,<sup>64</sup> and a frontal vulnerability in white matter anisotropy after TBI.<sup>65</sup> Despite this, little is known about the selective vulnerability of the components in the PFC circuit after TBI. Alterations in intrinsic excitability and membrane properties of pyramidal neurons have been reported in the mPFC acutely after a single diffuse brain injury associated with working memory deficits.<sup>66</sup> Axotomized pyramidal neurons in other areas of the cortex have also shown decreased firing rates acutely after injury.<sup>67</sup> However, no study to date has examined pyramidal neuron intrinsic excitability in the mPFC at a chronic time-point after repetitive head injury. We carefully assessed the firing response of layer V pyramidal neurons, the primary output neurons of the cortical microcircuit, to a series of hyperpolarizing and depolarizing current injections, and only a small decrease in the adaptation rate in rTBI mice was identified after repetitive injury. However, our data are limited by the possibility that we are grouping multiple unique sub-types of Layer V pyramidal neurons,<sup>68</sup> with a relatively low number of recordings if a large degree of heterogeneity exists in our population. There are a small number of sham neurons with a high degree of  $I_H$  current (Fig. 4D) and a larger adaptation index (Fig. 4J) that are not present in the rTBI population, raising this possibility. Nevertheless, a majority of the pyramidal neurons we recorded from appear to be sub-cortical projecting neurons, given the considerable  $I_H$  current in these cells<sup>35,68</sup>; the response to TBI might show different patterns in cortically projecting neurons, especially given the sensitivity of the corpus callosum to rTBI.<sup>69</sup> Future experiments using retrograde labeling to identify these distinct populations could be used to more carefully evaluate differences in response to injury. Alternatively, our sample might be composed of a mixture of neurons with intact and damaged axons; these populations have been noted to have a differential change in excitability after acute injury<sup>67</sup> and the presence of an axotomized population could explain the trend we noted for a decreased initial response to current injection, but further experiments are required to investigate this hypothesis. Finally, layer V pyramidal neurons may just show less response to injury compared with layer 2/3 pyramidal neurons in the mPFC,<sup>66</sup> a feature we have yet to test in this model of repetitive injury. At this point, only a slight decrease in adaptation rate is identified after rTBI, and extensive altered excitability of layer V pyramidal neurons in the mPFC is not a prominent feature of chronic mild rTBI.

Chronic microgliosis has been noted in many different models of rTBI, with various degrees of pathology described in the cortex, hippocampus, and/or white matter depending on the exact

model.<sup>25,50,51,53,70,71</sup> However, despite the importance of the mPFC in higher-order cognitive function, most analysis has been restricted to more caudal areas of the brain and the hippocampus closer to the area of injury impact. The mPFC in this model is far anterior from the area of direct impact (close to bregma); however, our results establish that diffuse mild repetitive injury that allows head movement and associated rotational acceleration of the brain does lead to chronic neuroinflammation both in the hippocampus as previously reported, as well as the mPFC, an area critically important for higher-order cognitive function.

Using T<sub>2</sub>-weighted MRI we have confirmed that this model of repetitive injury does not cause significant changes in brain structure similar to human repetitive injury.<sup>33–34</sup> Although T<sub>2</sub>-weighted MRI is ideal for structural analysis, it is not suitable for detecting axonal injury. With *ex vivo* diffusion tensor imaging and histological analysis, axonal injury has been identified in multiple white matter tracts one week after two repeated hits using the CHIMERA device with similar parameters.<sup>71</sup> Further work is required to assess how axonal injury progresses over time both in this model and in human injury, and which tracts are most susceptible to continued chronic degeneration.

In summary, we have identified that five repetitive mild head injuries in young mice cause chronic cognitive deficits in higher-order behaviors that are related to PFC function including working memory and social recognition. These deficits are accompanied by chronic microgliosis and a decrease in adaptation rate of layer V pyramidal neurons in the mPFC. Current studies are further addressing the impact of mild repetitive injury on the mPFC microcircuit, hippocampal-PFC axonal connections, and the role of sexual dimorphism in cognitive response after injury.

## Acknowledgments

This work was supported by research grants: NIH/NINDS R21NS096718, NIH/NINDS R21NS087458, NIH/NIA R01AG056770, CalBRAIN349087, NIH/NINDS R01NS095831, and a David Mahoney Neuroimaging Grant from the Dana Foundation (CA-0114728).

## Author Disclosure Statement

No competing financial interests exist.

## References

- Engberg, A.W., and Teasdale, T.W. (2004). Psychosocial outcome following traumatic brain injury in adults: a long-term population-based follow-up. *Brain Inj.* 18, 533–545.
- Ponsford, J., Draper, K., and Schonberger, M. (2008). Functional outcome 10 years after traumatic brain injury: its relationship with demographic, injury severity, and cognitive and emotional status. *J. Int. Neuropsychol. Soc.* 14, 233–242.
- Faul, M., Xu, L., Wald, M.M., and Coronado, V.G. (2010). Traumatic Brain Injury in the United States: Emergency Department Visits, Hospitalizations and Deaths 2002–2006. US Department of Health and Human Services, Centers for Disease Control and Prevention, National Center for Injury Prevention and Control. Available at: [www.cdc.gov/traumaticbraininjury/pdf/blue\\_book.pdf](http://www.cdc.gov/traumaticbraininjury/pdf/blue_book.pdf). Last accessed December 1, 2017.
- Vilkkki, J., Ahola, K., Holst, P., Ohman, J., Servo, A., and Heiskanen, O. (1994). Prediction of psychosocial recovery after head injury with cognitive tests and neurobehavioral ratings. *J. Clin. Exp. Neuropsychol.* 16, 325–338.
- Wallesch, C.W., Curio, N., Galazky, I., Jost, S., and Synowitz, H. (2001). The neuropsychology of blunt head injury in the early post-acute stage: effects of focal lesions and diffuse axonal injury. *J. Neurotrauma* 18, 11–20.



6. Bernstein, D.M. (2002). Information processing difficulty long after self-reported concussion. *J. Int. Neuropsychol. Soc.* 8, 673–682.
7. Mangels, J.A., Craik, F.I., Levine, B., Schwartz, M.L., and Stuss, D.T. (2002). Effects of divided attention on episodic memory in chronic traumatic brain injury: a function of severity and strategy. *Neuropsychologia* 40, 2369–2385.
8. Struchen, M.A., Clark, A.N., Sander, A.M., Mills, M.R., Evans, G., and Kurtz, D. (2008). Relation of executive functioning and social communication measures to functional outcomes following traumatic brain injury. *NeuroRehabilitation* 23, 185–198.
9. Stuss, D.T. (2011). Traumatic brain injury: relation to executive dysfunction and the frontal lobes. *Curr. Opin. Neurol.* 24, 584–589.
10. Spikman, J.M., Timmerman, M.E., Milders, M.V., Veenstra, W.S., and van der Naalt, J. (2012). Social cognition impairments in relation to general cognitive deficits, injury severity, and prefrontal lesions in traumatic brain injury patients. *J. Neurotrauma* 29, 101–111.
11. McMahon, P., Hricik, A., Yue, J.K., Puccio, A.M., Inoue, T., Lingsma, H.F., Beers, S.R., Gordon, W.A., Valadka, A.B., Manley, G.T., Okonkwo, D.O., and TRACK-TBI Investigators. (2014). Symptomatology and functional outcome in mild traumatic brain injury: results from the prospective TRACK-TBI study. *J. Neurotrauma* 31, 26–33.
12. McKee, A.C., Cantu, R.C., Nowinski, C.J., Hedley-Whyte, E.T., Gavett, B.E., Budson, A.E., Santini, V.E., Lee, H.S., Kubilus, C.A., and Stern, R.A. (2009). Chronic traumatic encephalopathy in athletes: progressive tauopathy after repetitive head injury. *J. Neuropathol. Exp. Neurol.* 68, 709–735.
13. Stern, R.A., Daneshvar, D.H., Baugh, C.M., Seichepine, D.R., Montenigro, P.H., Riley, D.O., Fritts, N.G., Stamm, J.M., Robbins, C.A., McHale, L., Simkin, I., Stein, T.D., Alvarez, V.E., Goldstein, L.E., Budson, A.E., Kowall, N.W., Nowinski, C.J., Cantu, R.C., and McKee, A.C. (2013). Clinical presentation of chronic traumatic encephalopathy. *Neurology* 81, 1122–1129.
14. Mez, J., Daneshvar, D.H., Kiernan, P.T., Abdolmohammadi, B., Alvarez, V.E., Huber, B.R., Alosco, M.L., Solomon, T.M., Nowinski, C.J., McHale, L., Cormier, K.A., Kubilus, C.A., Martin, B.M., Murphy, L., Baugh, C.M., Montenigro, P.H., Chaisson, C.E., Tripodis, Y., Kowall, N.W., Weuve, J., McClean, M.D., Cantu, R.C., Goldstein, L.E., Katz, D.I., Stew, R.A., Stein, T.D., and McKee, A.C. (2017). Clinicopathological evaluation of chronic traumatic encephalopathy in players of American football. *JAMA* 318, 360–370.
15. McKee, A.C., Stein, T.D., Kiernan, P.T., and Alvarez, V.E. (2015). The neuropathology of chronic traumatic encephalopathy. *Brain Pathol.* 25, 350–364.
16. Fleminger, S., Oliver, D.L., Lovestone, S., Rabe-Hesketh, S., and Giora, A. (2003). Head injury as a risk factor for Alzheimer's disease: the evidence 10 years on; a partial replication. *J. Neurol. Neurosurg. Psychiatry* 74, 857–862.
17. Chen, H., Richard, M., Sandler, D.P., Umbach, D.M., and Kamel, F. (2007). Head injury and amyotrophic lateral sclerosis. *Am. J. Epidemiol.* 166, 810–816.
18. Kang, J.H., and Lin, H.C. (2012). Increased risk of multiple sclerosis after traumatic brain injury: a nationwide population-based study. *J. Neurotrauma* 29, 90–95.
19. Jafari, S., Etmian, M., Aminzadeh, F., and Samii, A. (2013). Head injury and risk of Parkinson disease: a systematic review and meta-analysis. *Mov. Disord.* 28, 1222–1229.
20. Gardner, R.C., Burke, J.F., Nettiksimmons, J., Goldman, S., Tanner, C.M., and Yaffe, K. (2015). Traumatic brain injury in later life increases risk for Parkinson disease. *Ann. Neurol.* 77, 987–995.
21. Collins, M.W., Lovell, M.R., Iverson, G.L., Cantu, R.C., Maroon, J.C., and Field, M. (2002). Cumulative effects of concussion in high school athletes. *Neurosurgery* 51, 1175–1179; discussion 1180–1171.
22. Iverson, G.L., Gaetz, M., Lovell, M.R., and Collins, M.W. (2004). Cumulative effects of concussion in amateur athletes. *Brain Inj.* 18, 433–443.
23. Namjoshi, D.R., Cheng, W.H., McInnes, K.A., Martens, K.M., Carr, M., Wilkinson, A., Fan, J., Robert, J., Hayat, A., Crompton, P.A., and Wellington, C.L. (2014). Merging pathology with biomechanics using CHIMERA (Closed-Head Impact Model of Engineered Rotational Acceleration): a novel, surgery-free model of traumatic brain injury. *Mol. Neurodegener.* 9, 55.
24. Namjoshi, D.R., Cheng, W.H., Bashir, A., Wilkinson, A., Stukas, S., Martens, K.M., Whyte, T., Abebe, Z.A., McInnes, K.A., Crompton, P.A., et al. (2017). Defining the biomechanical and biological threshold of murine mild traumatic brain injury using CHIMERA (Closed Head Impact Model of Engineered Rotational Acceleration). *Exp Neurol* 292, 80–91.
25. Chen, H., Desai, A., and Kim, H.Y. (2017). Repetitive Closed-Head Impact Model of Engineered Rotational Acceleration Induces Long-Term Cognitive Impairments with Persistent Astroglia and Microglia in Mice. *J. Neurotrauma* 34, 2291–2302.
26. Wilk, J.E., Herrell, R.K., Wynn, G.H., Riviere, L.A., and Hoge, C.W. (2012). Mild traumatic brain injury (concussion), posttraumatic stress disorder, and depression in U.S. soldiers involved in combat deployments: association with postdeployment symptoms. *Psychosom. Med.* 74, 249–257.
27. Selassie, A.W., Wilson, D.A., Pickelsimer, E.E., Voronca, D.C., Williams, N.R., and Edwards, J.C. (2013). Incidence of sport-related traumatic brain injury and risk factors of severity: a population-based epidemiologic study. *Ann. Epidemiol.* 23, 750–756.
28. Petrie, E.C., Cross, D.J., Yarnykh, V.L., Richards, T., Martin, N.M., Pagulayan, K., Hoff, D., Hart, K., Mayer, C., Tarabochia, M., Raskind, M.A., Minoshima, S., and Peskind, E.R. (2014). Neuroimaging, behavioral, and psychological sequelae of repetitive combined blast/impact mild traumatic brain injury in Iraq and Afghanistan war veterans. *J. Neurotrauma* 31, 425–436.
29. Schwab, K., Terrio, H.P., Brenner, L.A., Pazdan, R.M., McMillan, H.P., MacDonald, M., Hinds, S.R., 2nd, and Scher, A.I. (2017). Epidemiology and prognosis of mild traumatic brain injury in returning soldiers: a cohort study. *Neurology* 88, 1571–1579.
30. Pellow, S., Chopin, P., File, S.E., and Briley, M. (1985). Validation of open/closed arm entries in an elevated plus-maze as a measure of anxiety in the rat. *J. Neurosci. Methods* 14, 149–167.
31. Leo, L.M., and Pamplona, F.A. (2014). Elevated plus maze test to assess anxiety-like behavior in the mouse. *Bio. Protoc.* 4, e1211.
32. Chou, A., Morganti, J.M., and Rosi, S. (2016). Frontal lobe contusion in mice chronically impairs prefrontal-dependent behavior. *PLoS One* 11, e0151418.
33. Moy, S.S., Nadler, J.J., Perez, A., Barbaro, R.P., Johns, J.M., Magnuson, T.R., Piven, J., and Crawley, J.N. (2004). Sociability and preference for social novelty in five inbred strains: an approach to assess autistic-like behavior in mice. *Genes Brain Behav.* 3, 287–302.
34. Feng X, Krubowski, K., Jopson, T., and Rosi, S. (2017). Delayed-matching-to-place task in a dry maze to measure spatial working memory in mice. *Bio. Protoc.* 7, pii: e2389.
35. Lee, A.T., Gee, S.M., Vogt, D., Patel, T., Rubenstein, J.L., and Sohal, V.S. (2014). Pyramidal neurons in prefrontal cortex receive subtype-specific forms of excitation and inhibition. *Neuron* 81, 61–68.
36. Sekerli, M., Del Negro, C.A., Lee, R.H., and Butera, R.J. (2004). Estimating action potential thresholds from neuronal time-series: new metrics and evaluation of methodologies. *IEEE Trans. Biomed. Eng.* 51, 1665–1672.
37. Cohen, J. (1988). *Statistical Power Analysis for the Behavioral Sciences*, 2nd ed. L. Erlbaum Associates: Hillsdale, NJ.
38. Shenton, M.E., Hamoda, H.M., Schneiderman, J.S., Bouix, S., Pasternak, O., Rathi, Y., Vu, M.A., Purohit, M.P., Helmer, K., Koerte, I., Lin AP, Westin CF, Kikinis R, Kubicki M, Stern RA, and Zafonte R. (2012). A review of magnetic resonance imaging and diffusion tensor imaging findings in mild traumatic brain injury. *Brain Imaging Behav.* 6, 137–192.
39. Wu, X., Kirov, I.I., Gonen, O., Ge, Y., Grossman, R.I., and Lui, Y.W. (2016). MR imaging applications in mild traumatic brain injury: an imaging update. *Radiology* 279, 693–707.
40. Gilmartin, M.R., Miyawaki, H., Helmstetter, F.J., and Diba, K. (2013). Prefrontal activity links nonoverlapping events in memory. *J. Neurosci.* 33, 10910–10914.
41. Yizhar, O., Fenno, L.E., Prigge, M., Schneider, F., Davidson, T.J., O'Shea, D.J., Sohal, V.S., Goshen, I., Finkelstein, J., Paz, J.T., Stehfest, K., Fudim, R., Ramakrishnan, C., Huguenard, J.R., Hegemann, P., and Deisseroth, K. (2011). Neocortical excitation/inhibition balance in information processing and social dysfunction. *Nature* 477, 171–178.
42. Zelikowsky, M., Hersman, S., Chawla, M.K., Barnes, C.A., and Fanselow, M.S. (2014). Neuronal ensembles in amygdala, hippocampus, and prefrontal cortex track differential components of contextual fear. *J. Neurosci.* 34, 8462–8466.
43. Bailes, J.E., Petraglia, A.L., Omalu, B.I., Nauman, E., and Talavage, T. (2013). Role of subconcussion in repetitive mild traumatic brain injury. *J. Neurosurg.* 119, 1235–1245.

44. Martins, A.T., Faisca, L., Esteves, F., Simao, C., Justo, M.G., Muresan, A., and Reis, A. (2012). Changes in social emotion recognition following traumatic frontal lobe injury. *Neural Regen. Res.* 7, 101–108.
45. Xiao, H., Jacobsen, A., Chen, Z., and Wang, Y. (2017). Detecting social-cognitive deficits after traumatic brain injury: an ALE meta-analysis of fMRI studies. *Brain Inj.* 31, 1331–1339.
46. Ubukata, S., Tanemura, R., Yoshizumi, M., Sugihara, G., Murai, T., and Ueda, K. (2014). Social cognition and its relationship to functional outcomes in patients with sustained acquired brain injury. *Neuropsychiatr. Dis. Treat.* 10, 2061–2068.
47. Klemenhagen, K.C., O'Brien, S.P., and Brody, D.L. (2013). Repetitive concussive traumatic brain injury interacts with post-injury foot shock stress to worsen social and depression-like behavior in mice. *PLoS One* 8, e74510.
48. Yu, F., Shukla, D.K., Armstrong, R.C., Marion, C.M., Radomski, K.L., Selwyn, R.G., and Dardzinski, B.J. (2017). Repetitive model of mild traumatic brain injury produces cortical abnormalities detectable by magnetic resonance diffusion imaging, histopathology, and behavior. *J. Neurotrauma* 34, 1364–1381.
49. Juengst, S.B., Kumar, R.G., Arenth, P.M., and Wagner, A.K. (2014). Exploratory associations with tumor necrosis factor-alpha, disinhibition and suicidal endorsement after traumatic brain injury. *Brain Behav. Immun.* 41, 134–143.
50. Mouzon, B.C., Bachmeier, C., Ferro, A., Ojo, J.O., Crynen, G., Acker, C.M., Davies, P., Mullan, M., Stewart, W., and Crawford, F. (2014). Chronic neuropathological and neurobehavioral changes in a repetitive mild traumatic brain injury model. *Ann. Neurol.* 75, 241–254.
51. Petraglia, A.L., Plog, B.A., Dayawansa, S., Chen, M., Dashnaw, M.L., Czerniecka, K., Walker, C.T., Viterise, T., Hyrien, O., Iliff, J.J., Deane, R., Nedergaard, M., and Huang, J.H. (2014). The spectrum of neurobehavioral sequelae after repetitive mild traumatic brain injury: a novel mouse model of chronic traumatic encephalopathy. *J. Neurotrauma* 31, 1211–1224.
52. Kondo, A., Shahpasand, K., Mannix, R., Qiu, J., Moncaster, J., Chen, C.H., Yao, Y., Lin, Y.M., Driver, J.A., Sun, Y., Wei, S., Luo, M.L., Albayram, O., Huang, P., Rotenberg, A., Ryo, A., Goldstein, L.E., Pascual-Leone, A., McKee, A.C., Meehan, W., Zhou, X.Z., and Lu, K.P. (2015). Antibody against early driver of neurodegeneration cis-P-tau blocks brain injury and tauopathy. *Nature* 523, 431–436.
53. Mouzon, B.C., Bachmeier, C., Ojo, J.O., Acker, C.M., Ferguson, S., Paris, D., Ait-Ghezala, G., Crynen, G., Davies, P., Mullan, M., Stewart, W., and Crawford, F. (2018). Lifelong behavioral and neuropathological consequences of repetitive mild traumatic brain injury. *Ann. Clin. Transl. Neurol.* 5, 64–80.
54. Yang, Z., Wang, P., Morgan, D., Lin, D., Pan, J., Lin, F., Strang, K.H., Selig, T.M., Perez, P.D., Febo, M., Chang, B., Rubenstein, R., and Wang, K.K. (2015). Temporal MRI characterization, neurobiochemical and neurobehavioral changes in a mouse repetitive concussive head injury model. *Sci. Rep.* 5, 11178.
55. Cheng, J.S., Craft, R., Yu, G.Q., Ho, K., Wang, X., Mohan, G., Mangnitsky, S., Ponnusamy, R., and Mucke, L. (2014). Tau reduction diminishes spatial learning and memory deficits after mild repetitive traumatic brain injury in mice. *PLoS One* 9, e115765.
56. Mannix, R., Meehan, W.P., Mandeville, J., Grant, P.E., Gray, T., Berglass, J., Zhang, J., Bryant, J., Rezaie, S., Chung, J.Y., Peters, N.V., Lee, C., Tien, L.W., Kaplan, D.L., Feany, M., and Whalen, M. (2013). Clinical correlates in an experimental model of repetitive mild brain injury. *Ann. Neurol.* 74, 65–75.
57. Zhang, J., Teng, Z., Song, Y., Hu, M., and Chen, C. (2015). Inhibition of monoacylglycerol lipase prevents chronic traumatic encephalopathy-like neuropathology in a mouse model of repetitive mild closed head injury. *J. Cereb. Blood Flow Metab.* 35, 706.
58. Dudchenko, P.A. (2004). An overview of the tasks used to test working memory in rodents. *Neurosci. Biobehav. Rev.* 28, 699–709.
59. McAllister, T.W., Sparling, M.B., Flashman, L.A., Guerin, S.J., Mammourian, A.C., and Saykin, A.J. (2001). Differential working memory load effects after mild traumatic brain injury. *Neuroimage* 14, 1004–1012.
60. Palacios, E.M., Sala-Llonch, R., Junque, C., Roig, T., Tormos, J.M., Bargallo, N., and Vendrell, P. (2012). White matter integrity related to functional working memory networks in traumatic brain injury. *Neurology* 78, 852–860.
61. Manktelow, A.E., Menon, D.K., Sahakian, B.J., and Stamatakis, E.A. (2017). Working memory after traumatic brain injury: the neural basis of improved performance with methylphenidate. *Front. Behav. Neurosci.* 11, 58.
62. Riga, D., Matos, M.R., Glas, A., Smit, A.B., Spijker, S., and Van den Oever, M.C. (2014). Optogenetic dissection of medial prefrontal cortex circuitry. *Front. Syst. Neurosci.* 8, 230.
63. Witt, S.T., Lovejoy, D.W., Pearson, G.D., and Stevens, M.C. (2010). Decreased prefrontal cortex activity in mild traumatic brain injury during performance of an auditory oddball task. *Brain Imaging Behav.* 4, 232–247.
64. Marquez de la Plata, C.D., Garces, J., Shokri Kojori, E., Grinnan, J., Krishnan, K., Pidikiti, R., Spence, J., Devous, M.D., Sr., Moore, C., McColl, R., Madden, C., and Diaz-Arrastia, R. (2011). Deficits in functional connectivity of hippocampal and frontal lobe circuits after traumatic axonal injury. *Arch. Neurol.* 68, 74–84.
65. Eierud, C., Craddock, R.C., Fletcher, S., Aulakh, M., King-Casas, B., Kuehl, D., and LaConte, S.M. (2014). Neuroimaging after mild traumatic brain injury: review and meta-analysis. *Neuroimage Clin.* 4, 283–294.
66. Smith, C.J., Xiong, G., Elkind, J.A., Putnam, B., and Cohen, A.S. (2015). Brain injury impairs working memory and prefrontal circuit function. *Front. Neurol.* 6, 240.
67. Greer, J.E., Povlishock, J.T., and Jacobs, K.M. (2012). Electrophysiological abnormalities in both axotomized and nonaxotomized pyramidal neurons following mild traumatic brain injury. *J. Neurosci.* 32, 6682–6687.
68. Kim, E.J., Juavinett, A.L., Kyubwa, E.M., Jacobs, M.W., and Callaway, E.M. (2015). Three types of cortical layer 5 neurons that differ in brain-wide connectivity and function. *Neuron* 88, 1253–1267.
69. Kinnunen, K.M., Greenwood, R., Powell, J.H., Leech, R., Hawkins, P.C., Bonnelle, V., Patel, M.C., Counsell, S.J., and Sharp, D.J. (2011). White matter damage and cognitive impairment after traumatic brain injury. *Brain* 134, 449–463.
70. Bolton Hall, A.N., Joseph, B., Brelsfoard, J.M., and Saatman, K.E. (2016). Repeated closed head injury in mice results in sustained motor and memory deficits and chronic cellular changes. *PLoS One* 11, e0159442.
71. Haber, M., Hutchinson, E.B., Sadeghi, N., Cheng, W.H., Namjoshi, D., Crompton, P., Irfanoglu, M.O., Wellington, C., Diaz-Arrastia, R., and Pierpaoli, C. (2017). Defining an analytic framework to evaluate quantitative MRI markers of traumatic axonal injury: preliminary results in a mouse closed head injury model. *eNeuro* 4.

Address correspondence to:

*Susanna Rosi, PhD*

*Zuckerberg San Francisco General Hospital*

*Building #1, Room 101*

*1001 Potrero Avenue*

*San Francisco, CA 94110*

*E-mail: susanna.rosi@ucsf.edu*